Architecture-Dependent Robustness and Bistability in a Class of Genetic Circuits

Jiajun Zhang,[†△] Zhanjiang Yuan,[†△] Han-Xiong Li,[‡] and Tianshou Zhou[†*]
[†]School of Mathematics and Computational Science, Sun Yat-Sen University, Guangzhou, China; and [‡]Department of Manufacturing, Engineering, and Engineering Management, City University of Hong Kong, Hong Kong

ABSTRACT Understanding the relationship between genotype and phenotype is a challenge in systems biology. An interesting yet related issue is why a particular circuit topology is present in a cell when the same function can supposedly be obtained from an alternative architecture. Here we analyzed two topologically equivalent genetic circuits of coupled positive and negative feedback loops, named NAT and ALT circuits, respectively. The computational search for the oscillation volume of the entire biologically reasonable parameter region through large-scale random samplings shows that the NAT circuit exhibits a distinctly larger fraction of the oscillatory region than the ALT circuit. Such a global robustness difference between two circuits is supplemented by analyzing local robustness, including robustness to parameter perturbations and to molecular noise. In addition, detailed dynamical analysis shows that the molecular noise of both circuits can induce transient switching of the different mechanism between a stable steady state and a stable limit cycle. Our investigation on robustness and dynamics through examples provides insights into the relationship between network architecture and its function.

INTRODUCTION

A challenge in systems biology is how to understand the relationship between genotype and phenotype, in which the genotype is determined by the information encoded in the DNA sequence and the phenotype by the context-dependent expression of the genome. Gene circuitry, which bridges the enormous divide between genotype and phenotype, is therefore to interpret the context and orchestrate the patterns of expression. The complexity is rooted either in an enormous variety of molecular mechanisms that are combined into complex genetic circuits or the diverse patterns of gene expression in response to environmental and developmental signals—or both. At present, it has become increasingly clear that our knowledge of even the well-studied organisms is still fragmentary and incomplete. We still lack the ability to predict the organism's response to a novel mutation in its gene sequence or to a novel compound in the environment.

The enormous diversity of molecular mechanisms and regulatory circuitry naturally raises a question about the base for the complex relationship between genotype and phenotype. Are these variations the result of historical accidents in the evolutionary process that happen to work well enough to survive selection? Or are they the result of natural selection to perform subtly different functions governed by some rules that can, in turn, help predict when a given design might evolve to perform a particular function in a specific context?

To our knowledge, there has not been a clear answer to this issue for natural systems thus far, but some exciting progress has been made. For example, Savageau and his colleagues (1–6) published a series of nice works to understand and/or elucidate the relationship between a fully characterized gene sequence and the phenotypic repertoire of an organism, and to conclude, therefore, some general design principles for elementary gene circuits. Related studies also include the work of Ma et al. (7), where they computationally searched all possible three-node enzyme network topologies to identify those that could perform adaptation, and found that only two major core topologies emerge as robust solutions. One was the proposal of a negative feedback loop with a buffering node and an incoherent feedforward loop with a proportioner node. The other possibility was from the work of Cagatay et al. (8), where they compared the *Bacillus subtilis* circuit that regulates differentiation into the competence state to an engineered circuit with an alternative architecture in silico and in vivo. Cagatay's group obtained some interesting results that reveal a tradeoff between temporal precision and physiological response range that is controlled by distinct noise characteristics of alternative circuit architectures.

Recently, genetic circuits with different regulatory patterns or topologies have been shown to generate similar dynamics and function (see (8) and the related references therein). This raises an equal question as to why a particular circuit topology is present in a cell when the same function can supposedly be obtained from an alternative architecture. This question is closed to robustness, as phenotypic robustness usually describes how variation on the level of genotype is translated into variation on the level of phenotype. Experimental investigation into it is challenging because biological circuits are typically comprised of many

Submitted February 9, 2010, and accepted for publication May 26, 2010.

△Jiajun Zhang and Zhanjiang Yuan contributed equally to this work.

*Correspondence: mcszhtsh@mail.sysu.edu.cn

Editor: Jason M. Haugh.

© 2010 by the Biophysical Society

0006-3495/10/08/1034/9 $2.00

doi: 10.1016/j.bpj.2010.05.036

components, some of which remain unknown. These components control physiological processes that are not fully understood. In addition, the processes themselves are behaviorally complex and therefore difficult to measure quantitatively. In contrast, theoretical investigations would become easy if simple modules with particular functions are considered. This is because mathematical models and computer modeling have been verified as powerful tools for analyzing simplified biological systems (9–15).

From a theoretical perspective, however, one must address three critical issues just as Alves and Savageau (2) pointed out:

1. Biologically meaningful behaviors must be identified or hypothesized and characterized by quantitative measures.
2. A representation of alternatives must be capable of describing the phenomenon of interest in quantitative terms.
3. Comparisons require analyses that explore biologically reasonable ranges of parameter values and use statistical methods to evaluate the results.

Based on the framework of Alves and Savageau's (2) handling issues and for simplicity, we selected two topologically equivalent genetic circuits of interlocked positive and negative feedback loops for investigation. (By topological equivalence, we mean that two circuits have the same path signs or loop gains, in which one gain is defined as the product of all regulatory signs in the path or loop with one positive/negative sign standing for activating/repressive regulation.) These two circuits, which are schematically shown in Fig. 1, are the native circuit (NAT circuit) and the circuit with an alternative architecture (ALT circuit), respectively.

The NAT circuit has been identified in many model organisms (16–21) and engineered through a synthetic biology method (22), whereas the ALT circuit has also been identified in some model organisms (see (23) and the related references therein) and has been studied theoretically (21,23). Such a selection is formed on the following molecular basis for construction of synthetic genetic circuits in *Escherichia coli* (see (24)): Both circuits consist of two components, denoted by *X* and *Y*, respectively. Component *X* acts as an autoactivator, thereby constituting a positive loop. However, it also activates *Y* that, in turn, represses *X* in the NAT circuit, which also represses *Y* that, in turn, activates *X* in the ALT circuit—thereby constituting a negative loop. Therefore, the ALT circuit can be viewed as a mutation of the NAT circuit with altered connectivity, implying that it can also be engineered in *E. coli* using a synthetic method (22,24). Because constitutive components of both circuits are known (8,9,12) and the structures are very simple, they may serve as a model system for studies aimed at understanding the relationship between genotype and phenotype.

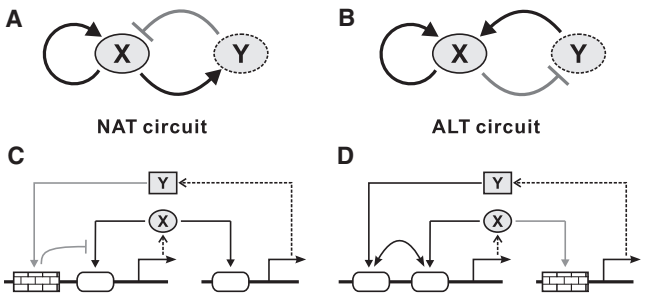

FIGURE 1 (*A* and *B*) Schematic of network structures for two gene regulatory circuits. (*C* and *D*) Their implementations at the level of transcription. In panel *D*, transcription factors *X* and *Y* regulate gene *x* through the cooperative AND-gate logic.

To show differences in robustness between two circuits, we performed global and local robustness analysis. By global robustness, we mean that it characterizes properties of a system's parameter region, such as the size or volume of oscillatory regions in the parameter space (25,26). In contrast, local robustness is the ability to maintain function in the face of external or internal environmental changes. It measures either the mean insensitivity of function characteristics (i.e., robust performance) or the persistence of a qualitative behavior (i.e., robust stability) in the presence of perturbations. For an oscillatory system, the robust performance mainly concerns the sensitivity of characteristics such as oscillation period and amplitude (27), whereas robust stability concerns the persistence of oscillations (28). The local robustness is an important property of biological systems (29), and has been studied extensively for diverse biological systems (30–32). We computationally searched for the oscillatory volume of the entire biologically reasonable parameter region for both circuit systems through large-scale random samplings, and found that the NAT circuit exhibits a distinctly larger fraction of the parameter region than the ALT circuit, indicating that the former has better global robustness than the latter. Regarding local robustness, we analyzed four different quantifiers, i.e., the mean parameter perturbation fraction, the mean maximal-Floquetier fraction, and the mean period and amplitude variance coefficients (see Methods for their meanings). The four quantifiers supplement to show the robustness difference between two circuits. Thus, the global and local robustness investigations altogether showed architecture-dependent robustness for the two circuits in the oscillation case, with the results indicating that the NAT circuit is superior to the ALT circuit.

We further analyzed dynamics of both circuits to show more differences between them. Interestingly, in contrast to what the genetic toggle switch system exhibits (33), we found that each circuit can exhibit bistability in the sense that both a stable steady state and a stable limit cycle are coexistent. The bistable characteristic of both circuits, however, is completely different. Whereas the NAT circuit has a unique,

stable, steady state located at the inside of the limit cycle in the phase space, the ALT circuit has three steady states—one is stable and the other two are unstable, with the stable steady state located at the outside of the limit cycle in the phase space. Moreover, the molecular noise of both circuits can induce transient switching between the two stable states. Such an investigation shows architecture-dependent bistability for the two circuits. This result, combined with the results by robustness analysis, provides insights into the relationship between network structure (genotype) and function (phenotype) for a class of genetic circuits.

MODELS AND METHODS

Models

Two gene circuits are schematically shown in Fig. 1. Note that Fig. 1, *A* and *B*, shows their network architectures, while Fig. 1, *C* and *D*, shows their implementations at the level of transcription. Note also that they are topologically equivalent, as both are composed of interlocked positive and negative feedback loops with the same loop gains. To derive our deterministic mathematical models, we integrated all biological processes such as transcription, translation, promoter binding, etc., into a single step, and used the standard quasi-steady-state equilibrium assumption that the mRNA molecule dynamics is much faster than the protein dynamics (34). To that end, we can arrive at the following set of differential equations for both circuits (see the Supporting Material):

$$\frac{dX}{dt} = \alpha_1 \frac{\beta_1 + X^n}{(K_1^n + X^n)(1 + (Y/K_2)^n)} - \lambda_1 X, \qquad \frac{dY}{dt} = \alpha_2 \frac{\beta_2 + X^n}{K_3^n + X^n} - \lambda_2 Y \tag{1}$$

$$\frac{dX}{dt} = \alpha_1 \frac{(\beta_1 + X^n)(\beta_2 + Y^n)}{(K_1^n + X^n)(K_2^n + Y^n)} - \lambda_1 X, \qquad \frac{dY}{dt} = \frac{\alpha_2}{1 + (X/K_3)^n} - \lambda_2 Y \tag{2}$$

Here X and Y represent the protein concentrations of the corresponding genes x and y. The value α_1 or α_2 is the maximum rate of the regulated expression (more precisely, the half-maximal expression arising at the concentration of X or Y equal to the Michaelis constant K_i ($i = 1, 2$, or 3), representing the strength of gene regulation). The values λ_i ($i = 1, 2$) are the degradation rate constants. The values β_i ($i = 1, 2$) represent the inverse of the fold-change of enhanced transcription rates when the promoter is occupied by the activator. The parameter n is the Hill coefficient (we assumed that all transcription factors are bound to operator sites in subunits of the same number). Note that we only considered that the transcription factors X and Y regulate gene x cooperatively (more precisely, through the cooperative AND-gate logic), and did not consider other possible regulation mechanisms (see (35,36) and the references therein).

The ranges of system parameters used in the simulation are set as $\alpha_i \in [10^{-2}, 1]$ (unit : molecules/s), $\lambda_i \in [10^{-5}, 10^{-2}]$ (unit : s^{-1}) $\beta_i = \rho_i K_i^n$ ($\rho_i \in [10^{-3}, 10^{-2}]$) with $i = 1,2$, and $K_j \in [10^2, 10^4]$ (unit : molecule) with $j = 1,2,3$. These are estimated (see the Supporting Material for details) according to the published parameter values for fundamental processes in gene expression (9,34,37–42), and n will take integer values of >1, but in most cases, we set $n = 2$.

Methods

Robustness analysis and its flow chart

Robustness, in the context of biological networks, broadly indicates that a system remains viable under different perturbations. Defining robustness in a precise form is a challenging task, given that robustness to different kinds of perturbations (e.g., environmental variation, molecular noise in chemical networks, or changes due to mutations) might involve different features of an existing network (26).

Conventional robustness analysis methods can be divided into two classes: global and local methods. Here, we give some comments on the existing robustness analysis methods.

First, the global robustness method mainly characterizes properties of a system's parameter space, such as the size or volume that allows the system to generate a dynamical behavior of interest (i.e., oscillation). Second, a parameter bifurcation diagram (14,43,44) often characterizes how qualitative properties of a system, such as the stability of steady states or attractors, changes as some of the model parameters are varied (45). The structure of a bifurcation diagram, however, can be influenced by changes in some of other parameters that may be not considered in bifurcation analysis, so this approach has limitations. Third, multivariate continuation methods (46) cannot show a strong advantage over unrestricted sampling for high-dimensional systems because they reduce the sampling space only by one dimension. Fourth, in contrast to global methods, most of local methods mainly analyze how perturbations affect a model behavior for a specified set of parameters (31,33,34).

The main limitation of the local methods is precisely this: they may not reflect the change of the model behavior under all possible parameter sets. Finally, we point out that most of robustness analysis methods in the literature are local (47). Examples include sensitivity analysis (48) that studies the effect of perturbations to a given set of parameters on model behavior, and its applications to circadian oscillators (27,49). Moreover, the local methods used are usually based on the linearization of a system and therefore hold for variations of only a few percent of the parameter values. Other works used stochastic simulations to estimate the robustness of a system to molecular noise (50). Efforts to extend a local analysis to systematic parameter variations in high dimensions (14,44) are often limited by computational cost. In addition, we point out that for a parameterized oscillatory system, different statistical tools can be applied to determine which parameters most affect its oscillatory behavior. Because parameter values for a particular function in a biological model are often constrained heavily within a bandwidth in the parameter space, this nature is useful in estimating oscillatory regions of parameter space. (Note that our numerical simulations showed that the oscillatory region for both circuits seems connected, so we did not consider the connectivity issue.) By comparing the shape and volume of oscillatory regions and susceptibility to specific parameter changes as well as the effect of molecular noise on amplitude and period, one should be able to show some differences in robustness between different oscillatory systems. This, in turn, can help predict the relationship between genotype and phenotype.

Here, we combined a global with a local method to analyze robustness of both circuits. More precisely, we introduced several geometrical indices to analyze the distribution of surface points in the parameter region that allows each circuit system to generate oscillations, and considered only such an oscillation case when analyzing robustness. For clarity, we used Fig. 2 to show the flow chart of our work. Simply speaking, for the above two mathematical models, we first sampled points in the parameter space to analyze global robustness; then we randomly perturbed each point in a certain parameter region to allow the system to produce oscillations for each periodic orbit for us to analyze local robustness; and finally, we computed variance coefficients to show the effect of molecular noise on amplitude and period. It should be pointed out that because a system's robustness depends on the shape and size of the parameter region that allows the system to generate a behavior of interest (26), it is necessary to separately investigate the global and local robustness (e.g., given the same volume for

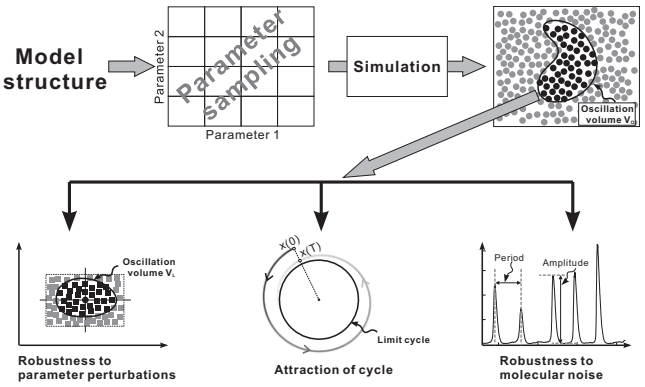

FIGURE 2 Flow chart of robustness analysis for parameterized oscillatory systems, where the arrow represents the flow direction.

a two-dimensional parameter region specified for the oscillation function, the circlelike region implies that the system is more robust in contrast to the rectanglelike region with a very small width).

Specifically, for each circuit, we used numerical simulation to assess its ability to perform oscillation function in a reliable fashion. For this, up to 1,000,000 ($M = 10^6$) parameter sets were sampled uniformly in logarithmic scale in the nine-dimensional parameter space (see Eq. 1 or 2, where the parameter n is fixed, e.g., $n = 2$) using the Latin hypercube sampling method (51). Thus, the first step of our approach involves the random sampling of a large set V, which can span the biologically feasible parameter space. Then, we found such points in V, which constitute a subset $V_0 \subset V$ (see Fig. 2), that for each point of V_0, the circuit system exhibits a stable sustained oscillation (to determine whether a system exhibits an oscillatory behavior, we gave a method in the Supporting Material by which a typical oscillation is displayed with an appropriate set of parameter values). Note that the volume occupied by the set V_0 only provides a first, crude characterization of the given circuit's robustness. To allow robustness comparison between the two models, we introduced a quantifier, which can measure the global robustness and is defined as $R_T = |V_0|/|V|$ (47). Therefore, the larger the R_T, the better the global robustness. For convenience, R_T is also called the "oscillation fraction".

Because the global robustness analysis does not show the persistence of a qualitative behavior of interest (e.g., oscillation), the next step of our method makes use of all identified viable parameter sets to carry out local robustness analysis. For this, we introduced four quantifiers (47) (explained below). To start, for each point in the set V_0, we let each component of the parameter vector be randomly perturbed N times (e.g., $N = 1000$) through the common Gaussian distribution with the zero mean at the same time, thus leading to a small region V_L (see also Fig. 2).

R_P. The quantifier R_P computes the fraction of the N parameter sets (i.e., the rate of the number of parameter sets that yield oscillatory behaviors over N). $\overline{R}_P$ computes the mean fraction for all the points in V_0. The index $\overline{R}_P$ describes a system's mean robustness to its parameter perturbations, which we therefore called the "mean parameter perturbation fraction". Note that the larger the $\overline{R}_P$, the better the local robustness.

R_A. The quantifier R_A similarly computes the fraction of the N parameter sets, i.e., the rate of the number of parameter sets that yield that the maximal norms of all Floquet multipliers (or Floquetiers for brevity) except for the unit norm Floquetier are <1 over N, and $\overline{R}_A$ then computes the mean fraction for all the points in V_0. For convenience, R_A is also called the "mean maximal-Floquetier fraction". It should be pointed out that R_A can describe robustness of a periodic orbit in the sense of Lyapunove stability because Floquetiers measure how fast the oscillator returns to its cycling behavior when its trajectory is transiently perturbed according to the Floquetier theory (52), and that its computation can be simplified (see the Supporting Material for details). Note that the smaller the $\overline{R}_A$, the better the local robustness.

σ_{per}, σ_{amp}. Finally, we quantified the effect of molecular noise on amplitude and period that altogether characterize oscillation. Given a set of molecular numbers and a reaction volume, Gillespie's algorithm (53) first generates a time series of each variable for each parameter set in V_0. Then, σ_{per} and σ_{amp} compute variance coefficients for period and amplitude based on this generated time series (see the Supporting Material for details). Furthermore, $\overline{\sigma}_{\text{per}}$ and $\overline{\sigma}_{\text{amp}}$ compute the averages of σ_{per} and σ_{amp} for all the points in V_0. For convenience, $\overline{\sigma}_{\text{per}}$ and $\overline{\sigma}_{\text{amp}}$ are called the "mean period coefficient" and the "amplitude variance coefficient", respectively. Note that the smaller the $\overline{\sigma}_{\text{per}}$ or $\overline{\sigma}_{\text{amp}}$, the better the robustness.

We emphasize that the four quantifiers, $\overline{R}_P$, $\overline{R}_A$, $\overline{\sigma}_{\text{per}}$, and $\overline{\sigma}_{\text{amp}}$, altogether can compensate for the deficiency of global robustness analysis in some cases, as mentioned above. In addition, we point out that $\overline{R}_A$ describes the robust stability whereas $\overline{R}_P$, $\overline{\sigma}_{\text{per}}$, and $\overline{\sigma}_{\text{amp}}$ describe robust performance (see Introduction).

Numerical computation

Simulations were performed using MATLAB 2009b (The MathWorks, Natick, MA). The system of ordinary differential equations was numerically solved by the subroutine ode45. To quantify robustness to molecular noise, we used the standard Monte Carlo technique, i.e., the famous Gillespie algorithm, to perform stochastic simulation (53).

RESULTS

Here, we combined the global with local robustness analysis methods to show architecture-dependent robustness for the above two models in the oscillation case. We presented results first on global robustness described by the oscillation fraction (R_T), and then on local robustness described by four quantifiers: $\overline{R}_P$, $\overline{R}_A$, $\overline{\sigma}_{\text{per}}$, and $\overline{\sigma}_{\text{amp}}$ (see Methods). In addition, we showed that both circuit systems exhibit bistability with different characteristics and that molecular noise can induce switching between a stable steady state and a stable limit cycle—an interesting dynamical phenomenon that, to our knowledge, is seldom found in biological systems.

Global robustness

We randomly sampled $M = 10^6$ parameter vectors covering an enormous range of several orders of magnitude for each parameter. The numerical results are shown in Fig. 3, *A* and *B*, where $n = 2$. Specifically, Fig. 3 *A* shows the viable volume fraction (R_T) for both circuit models, where the viable volume is interpreted as the average allowable variation per parameter that leaves the oscillation intact. From this figure, one can observe that R_T for the NAT circuit is significantly higher than that for the ALT circuit. More precisely, $R_T \approx 0.0083$ for the NAT circuit whereas $R_T \approx 0.0017$ for the ALT circuit, indicating that the former is approximately fivefold-times the NAT circuit. Fig. 3 *B* displays the distribution of oscillatory regions in the (λ_1, β_1) phase plane for both circuits, where one can observe that the NAT circuit exhibits greater robustness at low values of β_1 (this is possibly because of the dominant repression or degradation). Combining Fig. 3's panel *A* with panel *B* shows that the NAT circuit has much better global robustness than the ALT circuit.

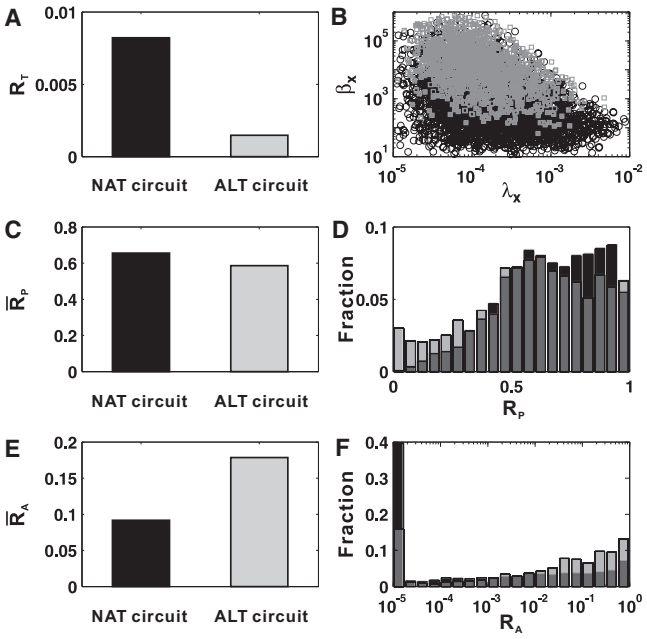

FIGURE 3 Results of robustness analysis for both circuit models. (*A*) The volume fraction (R_T) for both circuits. (*B*) The corresponding parameter regions that allow both circuit systems to generate oscillations in the (λ_x, β_x) phase plane, where $x = 1$. (*C*) The mean fraction for local random perturbations of parameters ($\overline{R}_P$). (*D*) The distribution of the fraction for local random perturbations of parameters (R_P). (*E*) The mean fraction for the maximal norm of two Floquet multipliers ($\overline{R}_A$). (*F*) The distribution of the fraction for the maximal norm of the Floquet multipliers (R_A). Here $n = 2$.

To test whether the conclusion depends on the sampling size, we also sampled other (e.g., $M = 10^5$) sets of parameters for each circuit. As done in Ma et al. (7), we defined a Q value as the number of sampled parameter sets that yield an oscillatory behavior. The Q values from the $M = 10^6$ samples and the $M = 10^5$ samples are highly correlated. We found that sampling with only $M = 10^5$ sets of parameters can identify most of oscillatory behavior, and that the global robustness of the NAT circuit is also much better than that of the ALT circuit, as the R_T of the NAT circuit is three-times larger than that of the ALT circuit in this case. In addition, we also tested whether the qualitative result depends on the Hill coefficient n and choice of parameter ranges. Some of these numerical results are shown in the Supporting Material, which indicate that our qualitative conclusion is unrelated to the choice of n and parameter ranges.

The above result on global robustness is the main argument to support the conclusion that the NAT circuit is more favored to implement the oscillation function than the ALT circuit. An intuitive explanation for this conclusion is as follows. With the NAT circuit, regardless of the strength of the positive link between X and Y, the negative feedback loop can always be established. With the ALT circuit, however, if the negative link between X and Y is weak (i.e., a large K_3 in Eq. 2), then the negative feedback loop is completely lost. This argument is consistent with the results in Fig. 3 *B*, where a high degradation rate and a low basal expression of X always cause the lost of oscillations in the ALT circuit. Furthermore, the ALT circuit is fragile to topological perturbations. The loss of the negative regulation can cause the runoff expression of X. On the other hand, it has theoretically been proven that the existence of a negative feedback is a necessary condition for a regulatory system to generate oscillations (13,23).

Local robustness

First, we used two quantifiers $\overline{R}_P$ and $\overline{R}_A$ (see Methods) to show differences in local robustness between two circuits (see Fig. 3, where the corresponding distributions are also displayed). Specifically, Fig. 3, *C* and *D*, shows the numerical results for $\overline{R}_P$ and the corresponding distribution, whereas Fig. 3, *E* and *F*, shows the numerical results for $\overline{R}_A$ and the related distribution. We observed from Fig. 3, *C* and *E*, that there is a small difference in $\overline{R}_P$ between two circuits, but there is a significantly large difference in $\overline{R}_A$. Because $\overline{R}_P$ and $\overline{R}_A$ for the NAT circuit are larger and smaller than those for the ALT circuit, respectively (Fig. 3, *C* and *E*), the former circuit has better local robustness than the latter. The corresponding distributions (Fig. 3) further verify this conclusion, e.g., at low values of β, the NAT circuit exhibits oscillation but the ALT circuit does not (Fig. 3 *B*).

Comparing Fig. 3's panel *C* with its panel *A*, we observed that a high average R_T leads to a high average $\overline{R}_P$. This would be due to connectivity of the oscillatory region for both circuits (the large-scale numerical simulations seem to have verified it). However, because of the different shape of the oscillatory region (Fig. 3 *B*), this would mean that the ALT circuit is more robust than the NAT circuit at $R_P = 1$ (Fig. 3 *D*). Note that there is a sudden jump at $R_A = 10^{-5}$ for both circuits (Fig. 3 *F*). This is mainly due to our statistical method. Because a number of Floquetiers' maximal norms are very small, we took them as the $R_A = 10^{-5}$ case when doing statistics, leading to a high fraction of Floquetiers' mean maximal norm for both circuits. In addition, we also perturbed each set of parameters in V_0 with a larger N, and computed the corresponding $\overline{R}_P$ and $\overline{R}_A$. The results still yield our conclusion (data not shown). In short, such an investigation on local robustness further supplements the conclusion obtained by analyzing global robustness.

Next, we turn to analyzing the effect of molecular noise on period and amplitude. For biochemical reactions, stochastic fluctuations (or molecular noise) are inevitable, as some molecular species are often present in small copy numbers. To capture the effect of the molecular noise, we computed the variance coefficient for fluctuated period and amplitude of each circuit (see Methods). Fig. 4 shows the related numerical results, where the Hill coefficient n is set as 2. As a whole, there is a small difference between two circuits because the two quantifiers $\overline{\sigma}_{\text{per}}$ and $\overline{\sigma}_{\text{amp}}$ have

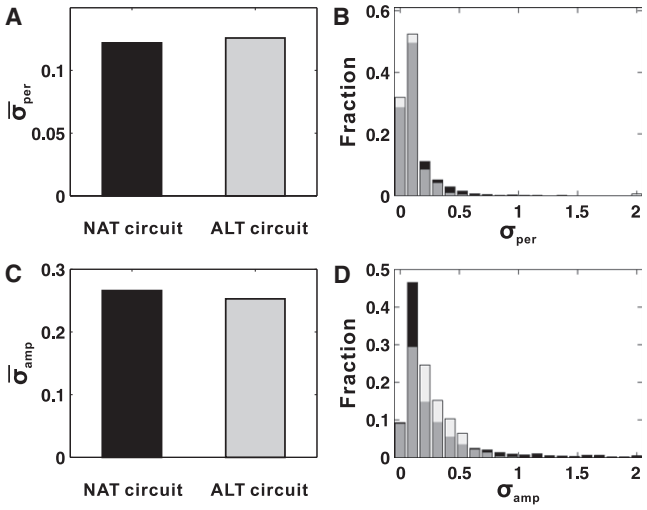

FIGURE 4 The effect of molecular noise on period and amplitude. (*A* and *B*) The mean variance coefficient and its distribution for period. (*C* and *D*) The mean variance coefficient and its distribution for amplitude. Here $n = 2$.

similar height (Fig. 4, *A* and *C*). The corresponding distributions (Fig. 4, *B* and *D*) show the small difference between two circuits. In fact, we observed from these two figures that the distribution of variance coefficient for period or amplitude is unimodal and has a similar shape. The numerical results in Fig. 4 indicates that altering connectivity in a genetic oscillator of coupled positive and negative feedback loops does not significantly change the robustness of its period and amplitude to molecular noise. In addition, to test whether this qualitative conclusion depends on n, we also computed $\overline{\sigma}_{\mathrm{per}}$ and $\overline{\sigma}_{\mathrm{amp}}$ for other integer values of n (data are not shown) and found that it is kept constant.

Despite this, it is worth noting that we can find many common parameter sets such that σ_{per} and σ_{amp} values for the NAT circuit are much larger than those for the ALT circuit, and can also find many common parameter sets such that σ_{per} and σ_{amp} values for the ALT circuit are much larger than those for the NAT circuit. In other words, for an arbitrarily given set of parameter values, we cannot determine which circuit has greater advantage in handling molecular noise over the other; as indicated in Fig. 4, the average effect is basically similar between the two.

The small difference in the mean variance coefficients between the two circuits would appear to stem from their having a topologically equivalent structure (i.e., coupled positive and negative feedback loops), and would be correlated with their inherent complex dynamics. This will be analyzed in the next subsection.

Bistability

The bistability in the conventional sense means that a dynamical system has two distinct stable steady states, and can exhibit a switch behavior under the excitation of external stimuli or molecular noise (54,55). Biological examples with this bistability include the λ-phage lysis-lysogeny switch (56,57), several mitogen-activated protein kinase cascades in animal cells (58), and cell-cycle regulatory CI circuits in *Xenopus* and *Saccharomyces cerevisiae* (54,15). Usually, bistable systems in the biological context are thought of as those involved in the generation of switch-like biochemical responses (58,59), the establishment of cell cycle oscillations and mutually exclusive cell cycle phases (15), the production of self-sustaining biochemical memories of transient stimuli (60), or the rapid lateral propagation of receptor tyrosine kinase activation (61).

Interestingly, the above two biological models can also exhibit bistability except for a simple behavior corresponding to the evolution toward a limit cycle for any initial conditions (refer to the Supporting Material). Here, the bistability means coexistence between a stable steady state and a stable limit cycle (i.e., two different kinds of attractors), where each stable state possesses its own basin of attraction—i.e., a region in the phase space from each point of which the system evolves toward this attractor. Such a coexistence phenomenon was previously found in chemical reactions (62) and in multipally regulated biochemical systems (63), and was studied mainly by Goldbeter et al. (64). We identified that both circuit systems have a different mechanism of generating bistable attractors that constitutes a so-called bistable oscillator (a complex oscillation mode). In theory, such a complex oscillation mode can be classified according to the number of steady states, namely:

Case 1. Coexistence of a stable limit cycle and a stable steady state in a multiple-steady-state situation (e.g., a stable steady state and a stable limit cycle are separated by the unstable manifold of a saddle point).

Case 2. Coexistence of stable limit cycle and a locally stable steady state in a unique-steady-state situation (e.g., the attracting basins of two attractors are separated by an unstable limit cycle).

For the NAT circuit, we found only Case 2 through adequate sampling of model parameters. Such a situation is also referred to as "hard excitation", by which the biological relevance of the switching behaviors was partially elucidated (64). Furthermore, we investigated the influence of molecular noise on switch behaviors, referring to Fig. 5, *A* and *B*, which shows a typical result. From this figure, we found that the molecular noise can constantly drive stochastic transitions between the stable steady state and the stable limit cycle. In contrast, for the ALT circuit, we numerically found only Case 1, and that molecular noise can also induce stochastic switching between the two stable states (Fig. 5, *C* and *D*). Such an effect of molecular noise on the bistable oscillator for both circuits was partially observed in a recent experiment (65). In addition, the PER-TIM model was shown to support the existence of

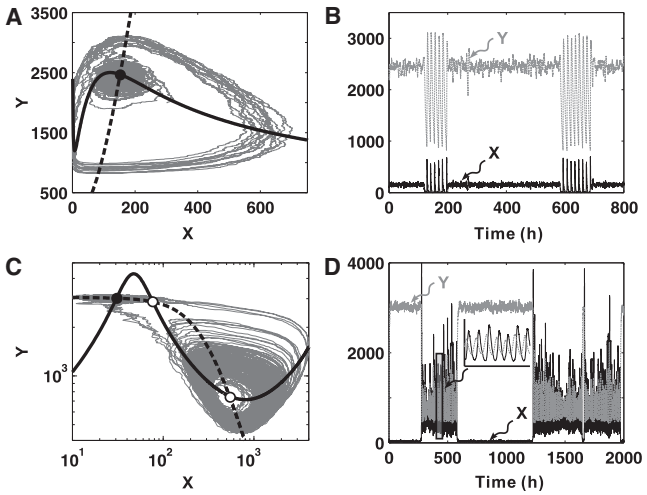

FIGURE 5 The bistability exhibited in two circuit systems, where a stable steady state and a stable limit are coexistent. (*A* and *B*) For the NAT circuit, where the parameter values are set as $\alpha_1 = 6.9568$ (mol/s), $\alpha_2 = 0.9018$ (mol/s), $\lambda_1 = 5.02429 \times 10^{-4}$ (s^{-1}), $\lambda_2 = 3.5042 \times 10^{-5}$ (s^{-1}), $K_1 = 0.121 \times 10^3$ (mol), $K_2 = 0.341 \times 10^3$ (mol), $K_3 = 0.472 \times 10^3$ (mol), $\beta_1 = 3.7 \times 10^{-3}$, and $\beta_2 = 2.1 \times 10^{-3}$. (*C* and *D*) For the ALT circuit, where the parameter values are set as $\alpha_1 = 2.8265$ (mol/s), $\alpha_2 = 0.3099$ (mol/s), $\lambda_1 = 3.6523 \times 10^{-4}$ (s^{-1}), $\lambda_2 = 1.0165 \times 10^{-5}$ (s^{-1}), $K_1 = 0.81 \times 10^3$ (mol), $K_2 = 1.3921 \times 10^3$ (mol), $K_3 = 0.306 \times 10^3$ (mol), $\beta_1 = 3.37 \times 10^{-3}$, and $\beta_2 = 2.87 \times 10^{-3}$. Panels *A* and *C* show the phase diagram for trajectories, where two nullclines (*dashed* and *solid curve*) and steady states (*solid circle* stands for the stable steady state; *open circles* represent unstable steady states) are also shown. Panels *B* and *D* show that molecular noise can induce a switch between two stable states, where, locally, an enlarged time series (*D*, *inset*) displays periodic motions of two components clearly. Here $n = 2$.

hard excitation, which may play a role in the mechanism of long-term suppression of circadian rhythms by light pulse (66). The biological relevance of the switching behaviors, however, is expected to require further elucidation.

The deeper dynamical analysis shows that the NAT circuit system can have both a unique stable steady and a stable limit cycle for a given set of parameter values; the ALT circuit system has, except for a stable limit cycle, three steady states (in which only one is stable; the other two are saddle and unstable focus, respectively). Moreover, for the NAT circuit, the stable steady state is located at the inside of the limit cycle; for the ALT circuit, it is located at the outside of the limit cycle in the phase space (see Fig. 5). The limit cycle is generated through bifurcation of the saddle node on invariant circle (67) for the NAT circuit system, but for the ALT circuit system, it is generated through a homoclinic bifurcation (data are not shown). Additionally, in our numerical simulations, we did not find the NAT circuit system to have a limit cycle similar to that exhibited by the ALT circuit system (or vice versa).

Note that in Global Robustness and Local Robustness (the above two subsections of Results), we did not concern ourselves with how a limit cycle is generated, but considered it insofar as a stable limit cycle was numerically found.

DISCUSSION AND CONCLUSIONS

We have shown that two circuits with topologically equivalent interlinking patterns of regulatory interactions can exhibit architecture-dependent robustness and bistability, which implies a closed relationship between genotype and phenotype. Moreover, our (global and local) robustness analysis has indicated that the NAT circuit is superior to the ALT circuit, from which we can reasonably speculate that the NAT circuit would have preferred natural selection compared to the ALT. Because both circuits are composed of interacting positive and negative loops, the most type of common network architecture in, e.g., biological circadian systems, our work is significant for understanding the core architectures of biological clocks, and helpful for understanding the related design principles in synthetic biology (22). However, we here point out that our robustness analysis cannot exclude the possibility that the ALT circuit exists in real biological systems, e.g., it can exist in a real biological system (see the example mentioned in Introduction, which implies that the ALT circuit would play a particular role that the NAT circuit cannot play if we consider it in the framework of the entire network).

Our deterministic models are simplified in some aspects; e.g., detailed biological processes such as transcription, translation, and promoter binding are combined into a single step, and we make the standard quasi-steady-state equilibrium assumption that the dynamics of the mRNA molecules is much faster than that of the proteins. Such a simplification, however, does not significantly affect our qualitative result (numerical computations were done but data were not shown). In addition, when doing stochastic simulation by using the Gillespie algorithm, we have also simplified the related biochemical reactions using Hill functions, e.g., each molecular species is modeled as a birth-death process with appropriate transition rates. But the stochastic simulation for the full biochemical reactions can show similar results (data not shown here), with the difference only in the case of a very small number of species molecules.

Regarding our robustness analysis, we here give some additional comments. As is well known, the way of generating a limit cycles may be different for different dynamical systems, and the usual bifurcation types include supercritical/subscriptical Hopf bifurcation, saddle node on invariant circle, homoclinic bifurcation, etc. Thus, oscillatory behavior in a neighborhood of the bifurcation point in general exhibits a poor robustness to perturbations. However, because our analysis method has used large-scale random samplings and several statistic indices (e.g., the oscillation fraction, the mean parameter perturbation fraction, the mean maximal Floquetier fraction, and the mean amplitude and period variance coefficients) to quantify the system robustness, our results on robustness are convincing. Also of note: The connectivity of parameter regions, which can yield a system capable of generating oscillations, is

a nonnegligible factor—but one which involves the description of more elaborate dynamics for which (to our knowledge) there has not been an available theory. Some biological systems could have multiconnected regions, but fortunately, such a case does not appear for our models, and moreover, our robustness analysis approach need not consider a connectivity issue.

From the viewpoint of dynamics, although we have shown some interesting dynamical behaviors (e.g., molecular noise can induce transient switching between a stable steady state and a stable limit cycle), the ALT circuit model merits further investigation. Such a phenomenon as we describe has not been investigated previously, to our knowledge. Perhaps, by investigating switch mechanisms for both circuits, one would find the essential relationship between genotype and phenotype, thus explaining why the NAT circuit architecture is selected to implement the oscillatory function. The corresponding investigations are underway, and some detailed results will be published elsewhere.

We wish to conclude with this comment: A biological system often contains many uncertain factors (e.g., some unknown system parameters). Thus, from the viewpoint of robustness as taken in this article, studying biological networks has practical significance. In this sense, our work provides a paradigm for other similar studies.

SUPPORTING MATERIAL

Two tables and three figures are available at http://www.biophysj.org/biophysj/supplemental/S0006-3495(10)00675-2.

The authors thank Dr. Marc Hafner for valuable discussions on numerical simulation.

This work was supported by grant Nos. 60736028, 30973980, and 2010CB945400 from the Natural Science Foundation of China, grant No. 20090460822 from the China Postdoctoral Science Foundation, and a grant from City University of Hong Kong (9360131).

REFERENCES

1. Savageau, M. A. 2001. Design principles for elementary gene circuits: elements, methods, and examples. *Chaos.* 11:142–159.
2. Alves, R., and M. A. Savageau. 2000. Comparing systemic properties of ensembles of biological networks by graphical and statistical methods. *Bioinformatics.* 16:527–533.
3. Coelho, P. M. B. M., A. Salvador, and M. A. Savageau. 2009. Quantifying global tolerance of biochemical systems: design implications for moiety-transfer cycles. *PLoS Comput. Biol.* 5:e1000319.
4. Savageau, M. A., P. M. B. M. Coelho, …, A. Salvador. 2009. Phenotypes and tolerances in the design space of biochemical systems. *Proc. Natl. Acad. Sci. USA.* 106:6435–6440.
5. Savageau, M. A. 1989. Are there rules governing patterns of gene regulation? *In* Theoretical Biology—Epigenetic and Evolutionary Order. B. C. Goodwin and P. T. Saunders, editors. Edinburgh University Press, Edinburgh, Scotland.
6. Wall, M. E., W. S. Hlavacek, and M. A. Savageau. 2004. Design of gene circuits: lessons from bacteria. *Nat. Rev. Genet.* 5:34–42.
7. Ma, W. Z., A. Trusina, …, C. Tang. 2009. Defining network topologies that can achieve biochemical adaptation. *Cell.* 138:760–773.
8. Cağatay, T., M. Turcotte, …, G. M. Süel. 2009. Architecture-dependent noise discriminates functionally analogous differentiation circuits. *Cell.* 139:512–522.
9. Süel, G. M., J. Garcia-Ojalvo, …, M. B. Elowitz. 2006. An excitable gene regulatory circuit induces transient cellular differentiation. *Nature.* 440:545–550.
10. Alon, U. 2006. Introduction to Systems Biology: Design Principles of Biological Circuits. CRC Press, Boca Raton, FL.
11. Shen-Orr, S. S., R. Milo, …, U. Alon. 2002. Network motifs in the transcriptional regulation network of *Escherichia coli*. *Nat. Genet.* 31:64–68.
12. Hasty, J., M. Dolnik, …, J. J. Collins. 2002. Synthetic gene network for entraining and amplifying cellular oscillations. *Phys. Rev. Lett.* 88:148101.
13. Snoussi, E. H. 1998. Necessary conditions for multistationarity and stable periodicity. *J. Biol. Syst.* 6:3–9.
14. Battogtokh, D., and J. J. Tyson. 2004. Bifurcation analysis of a model of the budding yeast cell cycle. *Chaos.* 14:653–661.
15. Cross, F. R., V. Archambault, …, M. Klovstad. 2002. Testing a mathematical model of the yeast cell cycle. *Mol. Biol. Cell.* 13:52–70.
16. Chen, K. C., L. Calzone, …, J. J. Tyson. 2004. Integrative analysis of cell cycle control in budding yeast. *Mol. Biol. Cell.* 15:3841–3862.
17. McAdams, H. H., and L. Shapiro. 2003. A bacterial cell-cycle regulatory network operating in time and space. *Science.* 301:1874–1877.
18. Cheng, P., Y. Yang, and Y. Liu. 2001. Interlocked feedback loops contribute to the robustness of the *Neurospora* circadian clock. *Proc. Natl. Acad. Sci. USA.* 98:7408–7413.
19. Ueda, H. R., M. Hagiwara, and H. Kitano. 2001. Robust oscillations within the interlocked feedback model of *Drosophila* circadian rhythm. *J. Theor. Biol.* 210:401–406.
20. Agrawal, S., C. Archer, and D. V. Schaffer. 2009. Computational models of the Notch network elucidate mechanisms of context-dependent signaling. *PLOS Comput. Biol.* 5:e1000390.
21. Tyson, J. J., K. C. Chen, and B. Novak. 2003. Sniffers, buzzers, toggles and blinkers: dynamics of regulatory and signaling pathways in the cell. *Curr. Opin. Cell Biol.* 15:221–231.
22. Stricker, J., S. Cookson, …, J. Hasty. 2008. A fast, robust and tunable synthetic gene oscillator. *Nature.* 456:516–519.
23. Novák, B., and J. J. Tyson. 2008. Design principles of biochemical oscillators. *Nat. Rev. Mol. Cell Biol.* 9:981–991.
24. Atkinson, M. R., M. A. Savageau, …, A. J. Ninfa. 2003. Development of genetic circuitry exhibiting toggle switch or oscillatory behavior in *Escherichia coli*. *Cell.* 113:597–607.
25. Eissing, T., F. Allgöwer, and E. Bullinger. 2005. Robustness properties of apoptosis models with respect to parameter variations and stochastic influences. *IEEE Syst. Biol.* 152:221–228.
26. Dayarian, A., M. Chaves, …, A. M. Sengupta. 2009. Shape, size, and robustness: feasible regions in the parameter space of biochemical networks. *PLOS Comput. Biol.* 5:e1000256.
27. Stelling, J., E. D. Gilles, and F. J. Doyle, 3rd. 2004. Robustness properties of circadian clock architectures. *Proc. Natl. Acad. Sci. USA.* 101:13210–13215.
28. Wang, R., L. Chen, and K. Aihara. 2007. Detection of cellular rhythms and global stability within interlocked feedback systems. *Math. Biosci.* 209:171–189.
29. Kitano, H. 2004. Biological robustness. *Nat. Rev. Genet.* 5:826–837.
30. Alon, U., M. G. Surette, …, S. Leibler. 1999. Robustness in bacterial chemotaxis. *Nature.* 397:168–171.
31. Yi, T. M., Y. Huang, …, J. Doyle. 2000. Robust perfect adaptation in bacterial chemotaxis through integral feedback control. *Proc. Natl. Acad. Sci. USA.* 97:4649–4653.
32. Ingolia, N. T. 2004. Topology and robustness in the *Drosophila* segment polarity network. *PLoS Biol.* 2:e123.

33. Gardner, T. S., C. R. Cantor, and J. J. Collins. 2000. Construction of a genetic toggle switch in *Escherichia coli*. *Nature*. 403:339–342.
34. Shahrezaei, V., and P. S. Swain. 2008. Analytical distributions for stochastic gene expression. *Proc. Natl. Acad. Sci. USA*. 105:17256–17261.
35. Zhang, J. J., Z. J. Yuan, and T. S. Zhou. 2009. Synchronization and clustering of synthetic genetic networks: a role for *cis*-regulatory modules. *Phys. Rev. E Stat. Nonlin. Soft Matter Phys.* 79:041903.
36. Zhang, J. J., Z. J. Yuan, and T. S. Zhou. 2009. Geometric characteristics of dynamic correlations for combinatorial regulation in gene expression noise. *Phys. Rev. E Stat. Nonlin. Soft Matter Phys.* 80:021905.
37. Hasty, J., F. Isaacs, …, J. J. Collins. 2001. Designer gene networks: towards fundamental cellular control. *Chaos.* 11:207–220.
38. McMillen, D., N. Kopell, …, J. J. Collins. 2002. Synchronizing genetic relaxation oscillators by intercell signaling. *Proc. Natl. Acad. Sci. USA*. 99:679–684.
39. Hooshangi, S., and R. Weiss. 2006. The effect of negative feedback on noise propagation in transcriptional gene networks. *Chaos.* 16:026108.
40. Wang, Y., C. L. Liu, …, P. O. Brown. 2002. Precision and functional specificity in mRNA decay. *Proc. Natl. Acad. Sci. USA*. 99:5860–5865.
41. Belle, A., A. Tanay, …, E. K. O'Shea. 2006. Quantification of protein half-lives in the budding yeast proteome. *Proc. Natl. Acad. Sci. USA*. 103:13004–13009.
42. Phillips, R., and R. A. Milo. 2009. A feeling for the numbers in biology. *Proc. Natl. Acad. Sci. USA*. 106:21465–21471.
43. Ma, L., and P. A. Iglesias. 2002. Quantifying robustness of biochemical network models. *BMC Bioinformatics.* 3:38.
44. Leloup, J. C., and A. Goldbeter. 2004. Modeling the mammalian circadian clock: sensitivity analysis and multiplicity of oscillatory mechanisms. *J. Theor. Biol.* 230:541–562.
45. Steuer, R., T. Gross, …, B. Blasius. 2006. Structural kinetic modeling of metabolic networks. *Proc. Natl. Acad. Sci. USA*. 103:11868–11873.
46. Henderson, M. E. 2002. Multiple parameter continuation: computing implicitly defined K-manifolds. *Int. J. Bifurcat. Chaos.* 13:451–476.
47. Hafner, M., H. Koeppl, …, A. Wagner. 2009. 'Glocal' robustness analysis and model discrimination for circadian oscillators. *PLOS Comput. Biol.* 5:e1000534.
48. Bagheri, N., J. Stelling, and F. J. Doyle, 3rd. 2007. Quantitative performance metrics for robustness in circadian rhythms. *Bioinformatics.* 23:358–364.
49. Rand, D. A., B. V. Shulgin, …, A. J. Millar. 2006. Uncovering the design principles of circadian clocks: mathematical analysis of flexibility and evolutionary goals. *J. Theor. Biol.* 238:616–635.
50. Gonze, D., J. Halloy, and A. Goldbeter. 2002. Robustness of circadian rhythms with respect to molecular noise. *Proc. Natl. Acad. Sci. USA*. 99:673–678.
51. Iman, R. L., J. C. Helton, and J. E. Campbell. 1981. An approach to sensitivity analysis of computer models, Part 1. Introduction, input variable selection and preliminary variable assessment. *J. Qual. Technol.* 13:174–183.
52. Khalil, H. K. 1996. Nonlinear Systems. Prentice-Hall, Upper Saddle River, NJ.
53. Gillespie, D. T. 1977. Exact stochastic simulation of coupled chemical reactions. *J. Phys. Chem.* 81:2340–2361.
54. Pomerening, J. R., E. D. Sontag, and J. E. Ferrell, Jr. 2003. Building a cell cycle oscillator: hysteresis and bistability in the activation of Cdc2. *Nat. Cell Biol.* 5:346–351.
55. Wang, J. W., J. J. Zhang, …, T. Zhou. 2007. Noise-induced switches in network systems of the genetic toggle switch. *BMC Syst. Biol.* 1:50.
56. Ptashne, M. 1992. A Genetic Switch: Phage and Higher Organisms. Cell Press/Blackwell Scientific Publications, Cambridge, MA.
57. Arkin, A., J. Ross, and H. H. McAdams. 1998. Stochastic kinetic analysis of developmental pathway bifurcation in phage λ-infected *Escherichia coli* cells. *Genetics.* 149:1633–1648.
58. Ferrell, Jr., J. E., and E. M. Machleder. 1998. The biochemical basis of an all-or-none cell fate switch in *Xenopus* oocytes. *Science.* 280:895–898.
59. Bhalla, U. S., P. T. Ram, and R. Iyengar. 2002. MAP kinase phosphatase as a locus of flexibility in a mitogen-activated protein kinase signaling network. *Science.* 297:1018–1023.
60. Lisman, J. E., and A. S. Mikhailov. 1985. A mechanism for memory storage insensitive to molecular turnover: a bistable autophosphorylating kinase. *Proc. Natl. Acad. Sci. USA*. 82:3055–3057.
61. Reynolds, A. R., C. Tischer, …, P. I. Bastiaens. 2003. EGFR activation coupled to inhibition of tyrosine phosphatases causes lateral signal propagation. *Nat. Cell Biol.* 5:447–453.
62. Aguda, B. D., L. L. H. Frisch, and L. F. Olsen. 1990. Experimental evidence for the coexistence of oscillatory and steady states in the peroxidase-oxidase reaction. *J. Am. Chem. Soc.* 112:6652–6656.
63. Decroly, O., and A. Goldbeter. 1982. Birhythmicity, chaos, and other patterns of temporal self-organization in a multiply regulated biochemical system. *Proc. Natl. Acad. Sci. USA*. 79:6917–6921.
64. Goldbeter, A., O. Decroly, …, F. Moran. 1988. Finding complex oscillatory phenomena in biochemical systems. An empirical approach. *Biophys. Chem.* 29:211–217.
65. Ushakov, O. V., H. J. Wünsche, …, M. A. Zaks. 2005. Coherence resonance near a Hopf bifurcation. *Phys. Rev. Lett.* 95:123903.
66. Leloup, J. C., and A. Goldbeter. 2001. A molecular explanation for the long-term suppression of circadian rhythms by a single light pulse. *Am. J. Physiol. Regul. Integr. Comp. Physiol.* 280:R1206–R1212.
67. Yang, D., Y. Li, and A. Kuznetsov. 2009. Characterization and merger of oscillatory mechanisms in an artificial genetic regulatory network. *Chaos.* 19:033115.